

Design of Brushless Permanent Magnet Motors – A Combined Electromagnetic and Thermal Approach to High Performance Specification

David G Dorrell

Dept of Electronics and Electrical Eng
The University of Glasgow
Glasgow G12 8LT
UK
d.dorrell@elec.gla.ac.uk

David A Staton

Motor Design Ltd
1 Eaton Court
Tetchill, Ellesmere, SY12 9DA
UK
dave.staton@motor-design.com

Malcolm I McGilp

Dept of Electronics and Electrical Eng
The University of Glasgow
Glasgow G12 8LT
UK
m.mcgilp@elec.gla.ac.uk

Abstract – This paper illustrates how modern design software packages can be linked together to aid the design of high specification electrical machines where the thermal rating and performance is critical. First the software is tested against the measured performance of an actual machine to validate accuracy of the linked electromagnetic and thermal software then various parameters are tested to illustrate the key points in producing a successful machine thermal design.

I. INTRODUCTION

A recent paper [1] on the thermal performance of a brushless permanent magnet motor illustrated that it is possible, with careful attention to the manufacturing techniques used to produce the machine, and the associated thermal resistances and capacitances, to obtain good steady-state and transient thermal performance prediction. Often the electromagnetic design is carried out using known parameters that should not be exceeded (e.g., a maximum winding current density of 5 to 7 A/mm²) then the thermal design is carried out once the electromagnetic design has been set. The thermal design then has set losses that can be used in a thermal network. This paper will illustrate that it is possible to do a combined electromagnetic and thermal design of a machine. This can reduce the material required, highlight localized hot-spots that need further attention in the design process, produce a tighter tolerance to the required IP rating and allow accurate re-rating of a machine when specifying a cyclic operating duty.

The paper then goes on to show how parameter variation, design changes, motor cooling and mounting can alter the machine performance and improve the machine operation. An example of a 6-pole brushless permanent magnet motor will be used to validate the design procedure and measurements on an actual machine will illustrate the software accuracy.

There are several books available which address the overall design of permanent-magnet electric machines [2]-[4] although the electromagnetic and magnetic material aspects rather than the thermal aspects take priority (but they are addressed).

Commercial software packages are now available for the electromagnetic design such as the suit of packages from the SPEED Laboratory, University of Glasgow [4]. They have some thermal modelling capabilities (multi-node network of up to 10 nodes) that can help with the initial sizing. For more sophisticated thermal modelling a software package dedicated to the thermal analysis of electrical machines can be used, e.g. Motor-CAD [5]. Both packages run under the

Windows OS and have full ActiveX capabilities. ActiveX is a standard method for linking programs together and transferring data. There is a dedicated link written using ActiveX technology to transfer geometric, loss and temperature data between the two programs. Macros can also be written in separate programs such as MATLAB or VBA to call both SPEED PC-BDC (brushless permanent magnet motor design software) and Motor-CAD. This is often done for more complex calculations such as automated optimisation, sensitivity analysis and the modelling of complex dynamic loads.

II. SOFTWARE AND VALIDATION

The software was first validated by testing against measurements from an actual machine where the motor parameters were either known or could be measured. The machine took the form of a 6-pole brushless permanent-magnet servo motor. The machine operated under ac control. The machine was tested using the fitted thermocouples. The specification of the machine is given below together with a description of the software arrangement. More detailed experimental results and comparisons are given in [1] however some comparisons for a cycling duty are also given below.

A. Machine Specification

The test machine is shown in Fig.1 It takes the form of a 6-pole brushless servo motor with surface-mounted SmCo magnets. The winding is 3-phase with 3 coils per phase giving a single layer winding with a coil pitch of 3 slots. The rated current was 6.1 A and the speed fixed at 2600 rpm. The frame size was 115 with an axial core length of 74 mm. The machine was flange mounted onto a simple aluminium plate which does not represent a good mounting so that it is to be expected that this machine will run slightly hot. This machine could be run under either ac or dc control, however it was decided to operate under ac control. This allowed the encoder to be rotated by nearly 90° elec. so that the current was almost on the d-axis. This meant that the machine could run at rated current but with no mechanical load, i.e., the machine was artificially loaded.

Five thermocouples were permanently attached to the machine. The first was in the centre of the winding, one was placed in the centre of a tooth, one was embedded in the casing, one was attached to the surface of the non-drive-end winding overhang and finally the fifth was attached to the non-drive-end end housing. A sixth was also used to measure the temperature of the shaft end when stationary. These were

logged using a data logger so that the temperatures could be continuously monitored during operation.



Fig. 1. Test Machine

B. Machine Models in PC-BDC and Motor Cad

The machine parameters were first put into the PC-BDC (in fact the manufacturer uses *SPEED* as their motor design database format so they were able to furnish a PC-BDC design file for this machine. Fig. 2 shows the cross section of the machine in PC-BDC. This geometry could be imported into Motor Cad and additional parameters, concerning things such as axial and radial casing and ducting, different types of cooling, gaskets between components and insulation and winding impregnation could be set. The cross-section and axial views in Motor Cad are shown in Figs. 3 and 4. Further details of the mechanical detailing and parameter adjustment are given in [1].

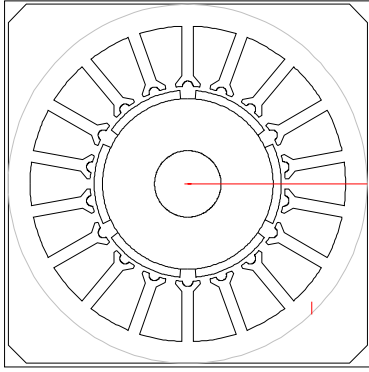


Fig. 2. Machine cross section from PC-BDC

C. Design Software Format

While [1] details the linking of the software it is worth noting some points here. PC-BDC is called from the Motor-CAD environment. The dialog that controls the data to be transferred is shown in Fig. 5. This link was developed by joint co-operation using Windows ActiveX (COM) software technology. Many CAD packages are exploring the use of software linkage; indeed *SPEED* software now links into several finite element packages and can act as the front-end geometrical input with the possibilities of developing further controls for the FEA from *SPEED*. Some FEA packages are

also offering specific calculation facilities such as induction motor leakage calculation in PC-IMD through direct linkage.

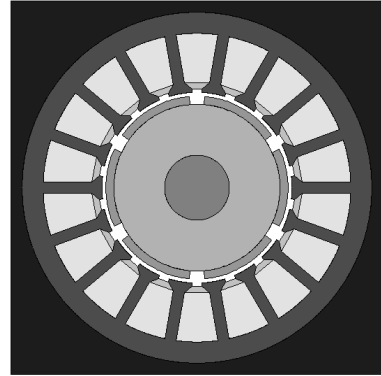


Fig. 3. Cross-section showing fining from Motor-CAD

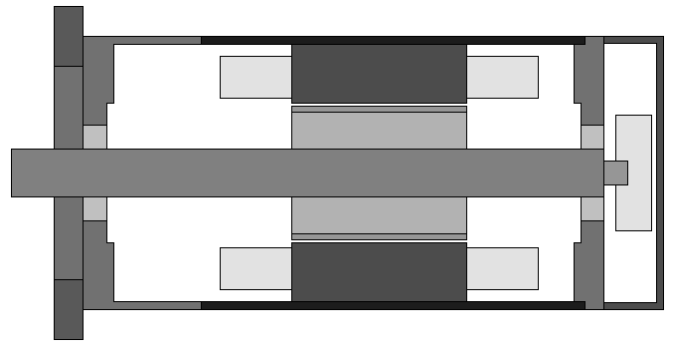


Fig. 4. Axial section

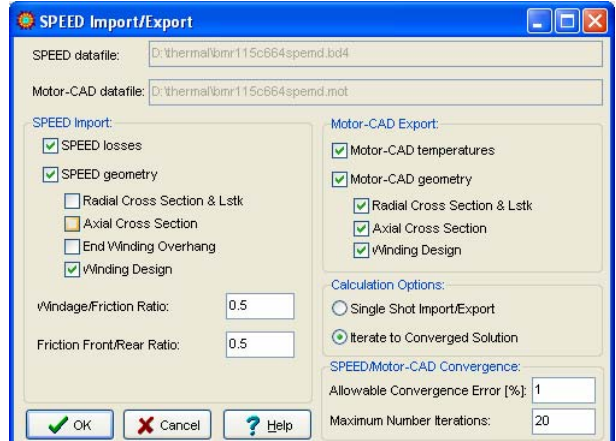


Fig. 5. *SPEED* link in Motor-CAD

D. Experimental Validation

Fig. 6 shows the comparison of simulated machine temperatures against measured for a duty cycle where the machine runs at rated current at 2600 rpm for the twenty minutes then it is switched on and off over successive ten minute intervals. This is shown for three locations – the winding, the stator tooth and the shaft. While the shaft seems to be incorrect this is because the temperature was measured using an uncalibrated hand-help thermometer and it is assumed that this was measuring about five degrees out in

absolute terms. Excellent correlation is found with the other temperature points. Only these three points are illustrated for clarity however the other points that were measured also showed good correlation similar to the winding and tooth temperature variation. These were given in [1].

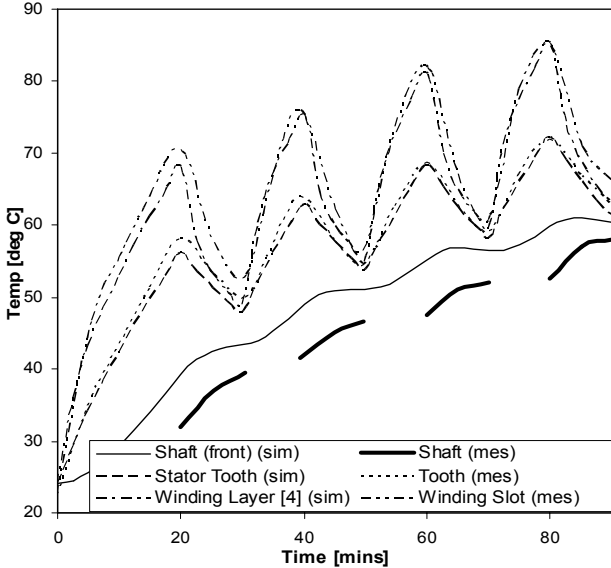


Fig. 6. Comparison between measured and simulated duty cycling

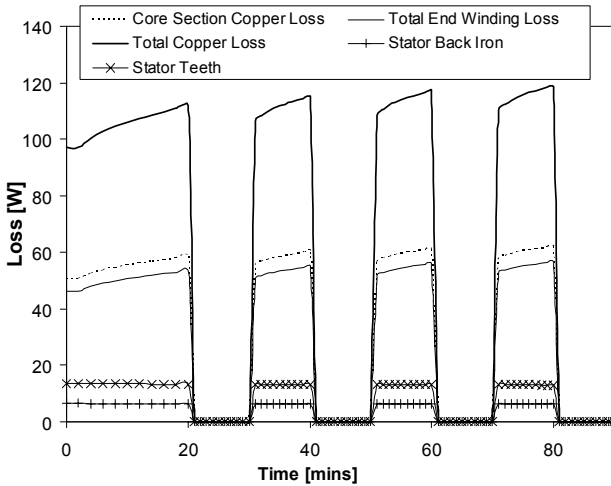


Fig. 7. Variation of machine loss with time

While [1] concentrated on the temperature variation it is also possible to obtain a breakdown of the losses within the machine and these are shown in Fig. 7. These are important to highlight the possible areas of design improvement. It can be seen that the losses are dominated by the copper loss. This is split into two – the losses in the slots and the end winding losses. The core loss is restricted to the stator and divided into tooth and yoke losses. The idea behind this is that it is now possible to identify where design improvements can be made; e.g., does the yoke or tooth width need to be increased or decreased or does the slot impregnation need to be improved or extra cooling put into the end winding regions. Also included is Fig. 8 which shows the variation of the magnet remanence B_r since this is an important issue for motor flux and torque production. In this case the machine

magnets are running quite cool and the magnetization is very stable. The remanence at 20 °C is 0.885 with a temperature coefficient of -0.045 %/°C. The steady-state magnet temperature at rated I_{ph} is 128 °C giving a B_r of 0.84. The temperature of the magnets are calculated using Motor-CAD while an iterative procedure is used to obtain the machine operating point where the magnetization and copper resistance and losses are varying with time.

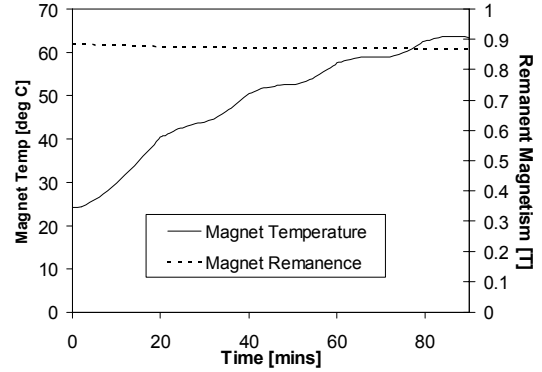


Fig. 8. Variation of magnet remanence with temperature

E. Thermal Network and Steady State Solution

The thermal network is shown in Fig. 9. This consists of many network components with a full set of thermal resistances for steady-state solution and thermal capacitances for transient solution. A full steady-state temperature solution is given in Table I.

In Table I it can be seen that the winding is the critical temperature component in a brushless PM machine. The losses are dominated by the copper loss and the active slot conductors are divided into several shells; also the front and rear end-winding sections are additional separate loss components. In Fig. 9 it can be seen that the vertical resistances tend to represent heat moving in the radial direction while horizontal resistances tend to represent heat moving in the axial direction.

III. PARAMETER VARIATION

We will first look at some simple parameter variations and how the motor temperature varies. We will focus on the temperature of the windings since this is the key point that can lead to thermal runaway. The machine itself was rated with Class F insulation. Therefore the machine has a thermal rating which specifies a maximum temperature of 155 °C and an ambient temperature up to 40 °C.

In this motor it is found that thermal runaway occurs in the stator windings. However this is not always the case and indeed thermal runaway can occur in the magnets; as the temperature increases, a reduction in magnetization occurs. If the machine is torque controlled then the controller will keep increasing the current, so that the motor temperature will keep increasing and a stable point is never obtained. Thermal runaway in the magnets can cause permanent demagnetization in the motor.

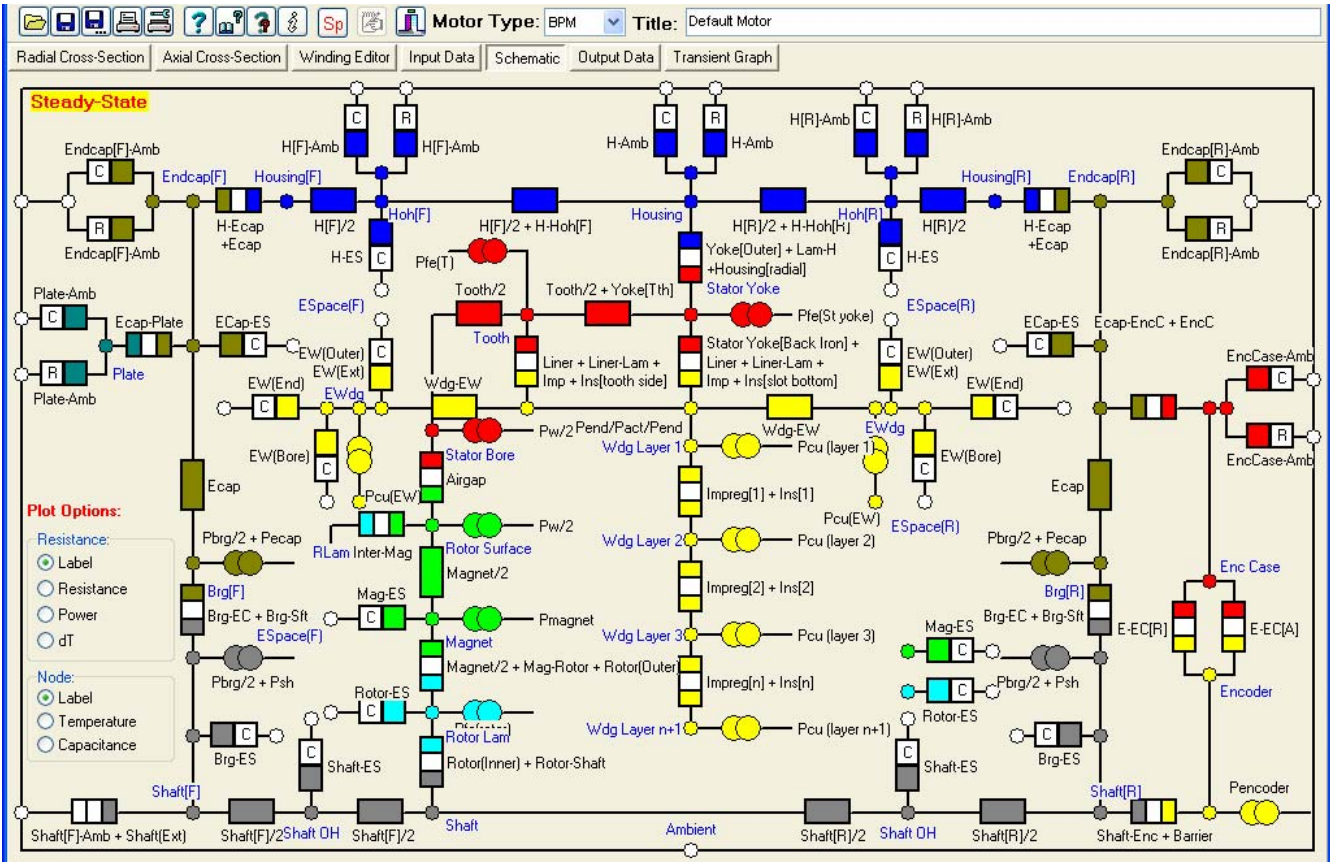


Fig. 9. Schematic of Thermal Network

TABLE I
STEADY STATE THERMAL SOLUTION

Thermal Node	Temp [deg C]	Thermal Node	Temp [deg C]
T [Ambient]	24.1	T [Shaft Ohang - Front]	124
T [Housing - Active]	117.8	T [Shaft - Front]	118.9
T [Housing-Overhang (F)]	113.6	T [Shaft Ohang - Rear]	126.9
T [Housing - Front]	111.3	T [Shaft - Rear]	124.9
T [Endcap - Front]	90.75	T[End Space - F]	125.3
T [Bearing - Front]	90.82	T[End Space - R]	127.7
T [Flange Mounted Plate]	88.15	T [Encoder]	128.9
T [Housing - Overhang (R)]	112.2	T [Encoder Case]	100.3
T [Housing - Rear]	109.7	T [Winding Average]	146.7
T [Endcap - Rear]	108.6	T [Active Winding Ave.]	146.8
T [Bearing - Rear]	108.7	T [End Winding Average]	146.6
T [Stator Lam (tooth)]	130.3	T [Winding Layer = 1]	144.3
T [Stator Lam (back iron)]	124.2	T [Winding Layer = 2]	146.8
T [Stator Surface]	130.2	T [Winding Layer = 3]	148.5
T [Rotor Surface]	128	T [Winding Layer = 4]	149.3
T [Magnet]	128	T [Winding Layer = 5]	149.4
T [Rotor Lamination]	127.9	T [EWdg (F)]	146.3
T [Shaft - Center]	127.8	T [EWdg (R)]	146.4

A. Temperature Variation with Mounting Plate and Load Attachment

The measurements were conducted with a small mounting plate. Many manufacturers assume that the mounting is a heat sink and we will illustrate this here. In Fig. 10 the mounting plate is changed. The actual plate is 140 mm

square, this is slowly increased in the simulation to 3000 mm square and the variation of the steady-state temperatures assessed. This illustrates that, for flange mounted machines, there is considerable cooling through the front mounting.

It is also possible to dissipate heat through the shaft. Therefore the front of the shaft can be locked down to a certain temperature. In this instance the shaft has a 30 mm extension. In Fig. 11 the front of the shaft extension is locked to 25 °C with a mounting plate of 140 mm square and 3000 mm square and compared to the temperatures when it is not attached to as load sink. It can be seen that while the winding temperature is pulled down slightly, it really only affects the local area around the front end shaft and bearing.

B. Overheating Via Excessive Ambient

The machine can overheat if the ambient becomes too high. This is illustrated in Fig. 12 where the ambient is increased and the steady-state temperatures are shown. The temperature ramps up at a constant rate.

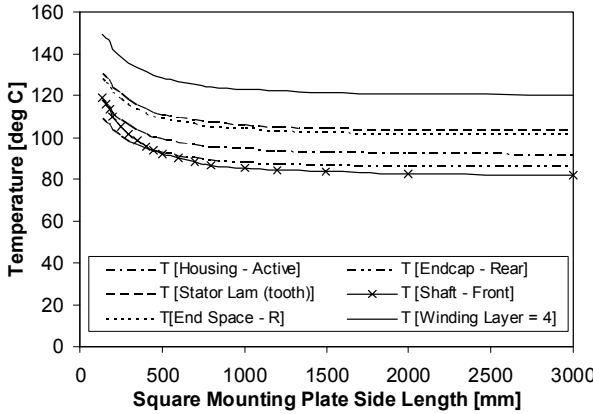


Fig. 10. Variation of temperature with mounting plate size

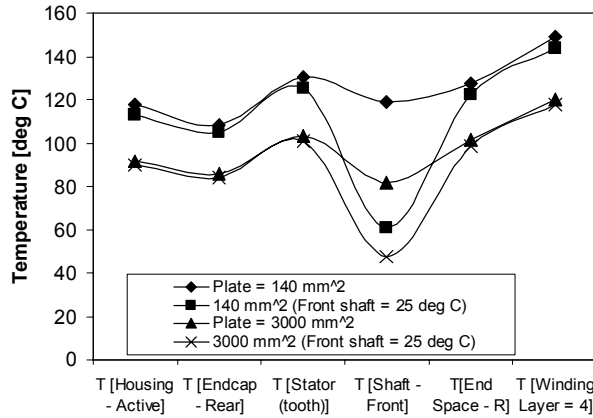


Fig. 11. Variation of temperature with mounting plate size and load attachment of front shaft

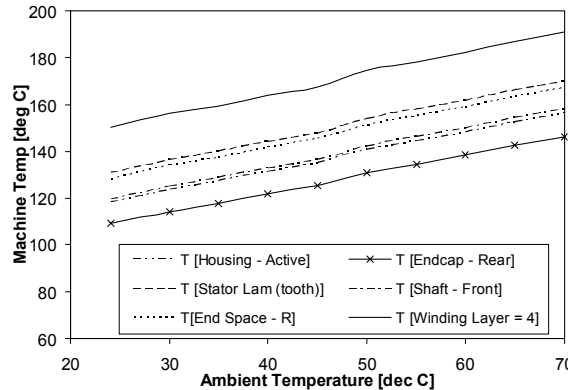


Fig. 12. Variation of machine temperatures with ambient

C. Overheating via Overload

The machine with the small plate mounting is marginal in terms of its thermal performance and rated current. We will now investigate its overload properties. At three times overload current (18.3 Arms) thermal runaway occurs so that the iterative procedure breaks down. In fact at 10 % error in convergence requires 28 iterations (the other simulations in this paper use 1 % error and converge in 2 to 5 iterations). This gives a winding temperature of 1890 °C which is clearly unreasonable, subsequent simulations do converge faster because the winding and magnet temperatures are set to the previous solution temperatures. With a further single shot solution this reduces to 1699 °C which is still quite close. At

these extremes convergence temperatures will vary depending on the starting temperatures. Fig. 13 shows the transient over the first 10 minutes, at 4 minutes the machine has already reached the thermal ratings and it is still steeply ramping up.

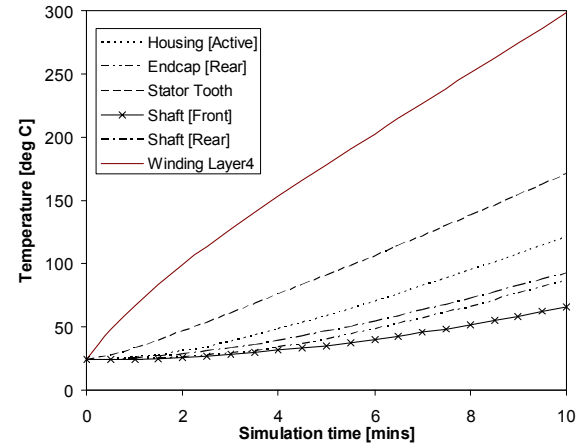


Fig. 13. Transient simulation with three times rated current

IV. DESIGN IMPROVEMENTS

A. Temperature Variation with Winding Impregnation

The winding impregnation can greatly affect the temperature distribution. There are several parameters that can be changed; here, however, we will concentrate on two parameters – the thermal conductivity of the impregnation resin (which is usually about 0.2 for standard resin but high performance ones are available which can be up to 1) and the impregnation goodness factor (which is an indication to the level of impregnation – in this machine it was found to be limited so that the goodness factor was set to 0.7). Table II shows the variation of the machine temperatures when the goodness is improved to 0.95 and then the impregnation conductivity is changes to 1 for both the resin and the wire insulation. It can be seen that there is a 9 °C reduction in winding temperature which can be important in a machine that is temperature critical.

TABLE II	
VARIATION OF WINDING LAYER 4 TEMP WITH IMPREGNATION	Winding Temp [°C]
Goodness = 0.7, conductivity = 0.2, wire insulation conductivity = 0.2	149.3
Goodness = 0.95, conductivity=0.2, wire insulation conductivity = 0.2	141.8
Goodness = 0.7, conductivity = 1, wire insulation conductivity = 0.2	141.9
Goodness = 0.95, conductivity = 1, wire insulation conductivity = 0.2	141.1
Goodness = 0.7, conductivity = 1, wire insulation conductivity = 1	140.4
Goodness = 0.95, conductivity = 1, wire insulation conductivity = 1	140.0

B. Temperature Variation with Gasket Thickness of Front Housing

It was found on dismantling the machine that a gasket was inserted between the front housing and the main casing which was about 0.25 mm thick. As a rule of thumb this sort of gasket has a thermal conductivity which is about ten times that of air so that it was represented as an air-gap of 0.025 mm. If this was removed and replaced by an air-gap of 0.05 mm (typical for a metal-metal joint without a conductive sealant) then the steady-state temperature of the winding

dropped from 149.7 °C to 147 °C while the front end-cap temperature increases from 90.7 °C to 97.9 °C.

C. Combined Improved Impregnation, Gasket Removal and Increased Mount Plate Size

If we use all the improved impregnation techniques in Section IV.A and remove the gasket discussed in Section IV.B then we can reduce the steady-state winding temperature to 136.3 °C in the slot which is now lower than the end windings temperature, which is 137.7 °C. We can also use a larger mounting plate (3m square) and this reduces the winding temperature to 96.4 °C. This illustrates that the a good reduction in steady-state temperature can be obtained by reducing series-connected thermal resistances together.

Further to this we can also look at the transient performance during overload as described in Section III.C where the there is three times over-current. This is shown in Fig. 14. The small iterative improvements in manufacturing lead to an improvement in the region of one minute until the thermal limit of the machine is reached when starting from cold. However, using the larger mounting plate seems to make little difference, it should be remembered that the convergence error is quite large with these simulations so accuracy will not be as good as at rated current.

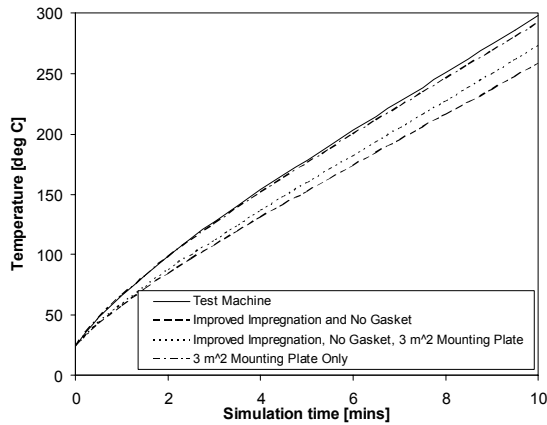


Fig. 14. Transient overload characteristics

D. Forced Cooling

The most common way to reduce the motor temperatures is to introduce forced air cooling. However space constraints prevents detailed discussion of this here however, simply by introducing a forced air-flow over the machine casing of 5 m/s then the winding temperature can be reduced from 149.7 °C to 108.1 °C which clearly shows that this is the most effective way to reduce the motor temperature. If forced-air cooling is used in conjunction with the impregnation improvement and large 3000 mm square mounting plate then the steady-state winding temperature is now even lower at 79.7 °C.

In terms of the transient performance, Fig. 15 shows the winding temperature over the first ten minutes with natural cooling and forces air cooling without any change in machine geometry. It appears that the forced-air cooling actually has little effect on the initial transient performance.

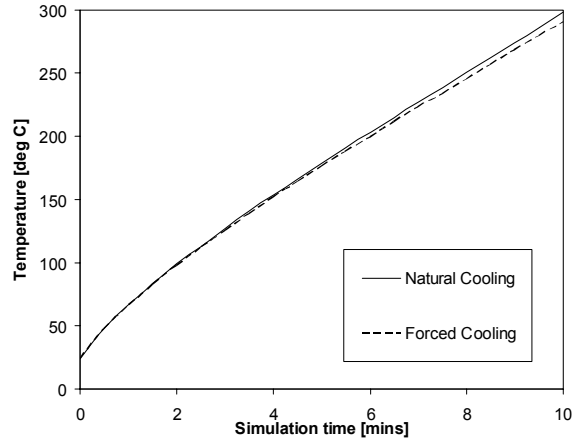


Fig. 15. Transient overload characteristics – comparison between natural and forced air cooling

V. CONCLUSIONS

This paper illustrates that it is possible to accurately model the thermal performance of an electrical machine using linked electromagnetic and thermal simulation software. This was verified experimentally and the machine was found to be marginal in terms of its thermal rating when mounted on a light mounting plate. It was then demonstrated that the machine would run cooler if mounted on a larger plate and then various small design changes illustrated several methods than can be used to improve the thermal performance if it is marginal.

The transient overload performance was also addressed, which is important when considering the machine tolerance to overloading. It was also illustrated that force air cooling is a very effective way to improve the machine steady-state thermal performance, even without changing the machine design but it is less effective on a transient overload.

VI. REFERENCES

- [1] D. G. Dorrell, D. A. Staton, J. Kahout, D. Hawkins and M. I. McGilp, "Linked Electromagnetic and Thermal Modelling of a Permanent Magnet Motor", *IEE Power Electronics, Machines and Drives Conference, Dublin, April 2006*.
- [1] J. R. Ireland, *Ceramic Permanent-Magnet Motors*, New York, McGraw-Hill Book Company, 1968.
- [2] J. R. Hendershot, T. J. E. Miller, *Design of Brushless Permanent-Magnet Motors*, Oxford, Clarendon Press, 1994.
- [3] L. R. Moskowitz, *Permanent magnet Design and Application Handbook*, Florida, Krieger Publishing Company, 1995.
- [4] TJE Miller, *SPEED's Electrical Motors*, SPEED Laboratory, University of Glasgow 2004.
- [5] D. A. Staton, Motor-CAD V2, Motor Design Ltd, October 2005.